NASA Technical Paper 1380

Theoretical Study of VTOL Tilt-Nacelle Axisymmetric Inlet Geometries

J. Dennis Hawk and Norbert O. Stockman

JANUARY 1979

NASA

NASA Technical Paper 1380

Theoretical Study of VTOL Tilt-Nacelle Axisymmetric Inlet Geometries

J. Dennis Hawk and Norbert O. Stockman
Lewis Research Center
Cleveland, Ohio

National Aeronautics
and Space Administration

**Scientific and Technical
Information Office**

1979

SUMMARY

This report presents a systematic, theoretical study of the inlet design parameters of VTOL tilt-nacelles. The parameters considered are internal-lip contraction ratio, internal-lip major-to-minor axis ratio, diffuser-exit-area to throat-area ratio, and maximum diffuser wall angle and shape. Each of the inlets presented herein was analyzed at the same given flow condition of free-stream velocity, angle between the free-stream and centerline of the inlet, and diffuser-exit Mach number. The effects of these geometric parameters on surface static-pressure distribution, peak surface Mach number, diffusion velocity ratio, and the tendency for the inlet flow to separate are presented.

INTRODUCTION

Lift cruise fans in tilt nacelles are being considered for VTOL (vertical takeoff and landing) aircraft. The inlets of these types of nacelles are subjected to wide ranges of incidence angles, flight speeds, and throttle settings during takeoff, landing, and cruise. The inlet design is of major concern because at large angles of attack the inlet internal flow may separate. Separated flow increases distortion, which causes fan-blade stress and may cause core-compressor stall. Separation-free internal flow is largely a function of the inlet internal design. The external-lip geometry must be compatible with the internal-lip design and must be designed to avoid drag rise at cruise. The inlet should be as small in diameter and as short as possible to minimize friction drag and weight. Therefore, the inlet design becomes a compromise between the internal and external lip shapes for the best low-speed and cruise performance.

It is the purpose of this report to present the effect of pertinent geometric variables on the aerodynamic performance of axisymmetric inlets applicable to tilt-nacelle VTOL aircraft. The geometric parameters investigated were internal-lip contraction ratio, internal-lip major-to-minor axis ratio, diffuser-exit-area to throat-area ratios, and maximum diffuser wall angle and shape.

These geometric variables are investigated at a selected severe flight condition for their effect on the following dependent quantities: the surface static-pressure distribution, peak surface Mach number, diffusion velocity ratio (ratio of maximum to minimum surface velocity), separation location, and external surface area.

SYMBOLS

A	area
a	major axis of internal lip (fig. 1)
b	minor axis of internal lip (fig. 1)
C_F	skin friction
CR	contraction ratio
D	diameter
L	length of inlet (fig. 1)
M	Mach number
P	pressure
R	radius
S	local surface distance
S_{ref}	surface distance from inlet highlight to diffuser exit
S_{stag}	surface distance from stagnation point to diffuser exit
V	velocity
x	axial distance
$\overline{x}$	external forebody length (fig. 1)
y	radial distance from inlet highlight
$\overline{y}$	external forebody thickness (fig. 1)
α	incidence angle of inlet, angle between free-stream velocity and inlet axis (fig. 1)
θ	inlet circumferential position
λ	maximum wall angle

Subscripts:

c	centerbody
d	diffuser
dd	drag divergence
e	exit
h	highlight

max	maximum
min	minimum
s	static
stag	stagnation point
sur	external surface
t	throat
tot	total
0	free stream

DESCRIPTION OF INLET GEOMETRIES

The nomenclature used to define the inlet geometry is shown in figure 1. The geometric variations of the inlets investigated are shown in figures 2 to 5.

Baseline Configuration

The baseline inlet consists of the baseline lip and the baseline diffuser (inlet 1 in fig. 2). The baseline internal-lip profile was an ellipse with a major-to-minor axis ratio a/b of 2.0 and an inlet contraction ratio (defined as the ratio of highlight area to throat area $(D_h/D_t)^2$) of 1.56.

The baseline external-forebody profile was a bisuperellipse curve of the form (ref. 1)

$$\left(\frac{x}{\bar{x}}\right)^{1.77} + \left(\frac{y}{\bar{y}}\right)^{2.246} = 1$$

The external forebody length-to-maximum diameter ratio ($\bar{x}/D_{max} = 0.266$) was not varied. The value of this parameter was selected for the prescribed value of drag-divergence Mach number of 0.8 (ref. 2).

The baseline diffuser had a cubic wall with a maximum wall angle of 8.7° at its midpoint. The baseline diffuser-exit-area to throat-area ratio was 1.10. This resulted in a design throat Mach number of 0.72 for a design diffuser-exit Mach number of 0.6.

The same centerbody was used for all inlets analyzed. The highlight of the centerbody was located at a point $x/R_d = 0.86$ from the diffuser exit. The centerbody profile was a superellipse curve of the form

$$\left(\frac{x}{\bar{x}}\right)^{1.72} + \left(\frac{y}{\bar{y}}\right)^{1.72} = 1$$

At the diffuser exit $y/R_d = 0.46$.

Geometric Variations

Only one inlet geometric parameter was varied at a time. For lip design changes, the baseline diffuser was used, and, for diffuser design changes, the baseline lip was used.

The contraction ratio of the lip was varied from 1.56 (baseline) to 1.46 and 1.69 (inlets 2 and 3, fig. 2).

The lip a/b ratio was varied from 2.00 (baseline) to 1.75, 1.50, and 1.25 (inlets 4 to 6, fig. 3).

The diffuser-exit-area to throat-area ratio A_{de}/A_t was varied from the baseline 1.10 to 1.00 and 1.14 (inlets 7 and 8, fig. 4).

The maximum diffuser wall angle was varied from the nominal value of 8.7° to 12° and 14° (inlets 9 and 10, fig. 5). For each of these maximum wall angles, the diffuser wall was changed from a cubic to a conic design (inlets 11 to 13, fig. 5). The conic segment was mated to the fan face with a circular arc and to the lip with an elliptical section with an a/b ratio of 3.0.

A summary of the geometric variables is presented in table I.

METHOD OF ANALYSIS

Selection of Study Flow Condition

The inlet incidence angle and throat Mach number (as determined by engine throttle setting) as a function of free-stream velocity during a typical landing approach are shown in figure 6 (from ref. 3) for a subsonic, VSTOL, tilt-nacelle aircraft, with and without a jet deflection vane in the exhaust jet. These data have been interpreted in terms of parameters pertinent to inlet aerodynamics (solid lines in fig. 7) and are compared with the experimental separation bound for a 1.56-contraction-ratio inlet (dashed line).

Based on figure 7 a typically severe flow condition (the data symbol) was selected for analysis. This condition occurred at a free-stream Mach number of 0.18, an incidence angle of 60°, and a diffuser-exit Mach number of 0.357.

Potential Flow Analysis

The theoretical potential flows at the operating conditions for the various inlets were obtained using the calculational procedures for the axisymmetric inlets described in reference 4. Briefly, the elements of the potential-flow computer-program system are (1) a program for geometry definition, (2) an incompressible potential-flow calculation program, and (3) a program to combine basic potential-flow solutions into solutions having specified values of free-stream velocity, incidence angle, and inlet mass flow, and also to correct the results for compressibility effects and local, supersonic-Mach-number effects.

The potential-flow calculations were used to obtain surface-pressure distributions, peak Mach numbers, and diffusion velocity ratios for the inlet geometries. All potential-flow results shown, except for the circumferential variations of surface V_{max}/V_{de}, are for the windward side of the inlet ($\theta = 0^{o}$) since the most severe flow conditions occur there.

Viscous Flow Analysis

The theoretical viscous effects (boundary layer) for the inlets were obtained using a calculation procedure as prescribed by Cebeci (ref. 5). In this procedure a finite-difference technique is used to solve the governing boundary-layer equations. From this procedure, the internal-flow separation point was taken to be the point where the skin friction went to zero. A typical skin friction plot for the baseline inlet is shown in figure 8. The first segment of the curve, to the minimum at about $S/S_{stag} = 0.24$, is in the laminar flow region. The next segment, which ends at the local maximum, is the transition from laminar to turbulent flow. The flow after that point until separation (skin friction $C_F = 0$) is turbulent. All inlets analyzed in this study that separated did so in the turbulent range.

RESULTS AND DISCUSSION

In this section the results will be presented as plots of surface-pressure distribution, diffusion velocity ratio, and external surface area, all as functions of the geometric variables.

Surface-pressure distributions are shown because they permit easy comparison of the nature of the adverse pressure gradients for the several geometries.

Reference 6 established that two parameters readily obtained from potential flow are useful in determining if separation will occur. These are (1) the diffusion velocity

ratio, defined as the ratio of the maximum to the minimum surface velocities, and (2) the peak surface Mach number. For many of the inlet geometries the minimum surface velocity is essentially the diffuser-exit velocity. At low average throat Mach numbers (below 0.6), the inlet flow appears to be diffusion limited; that is, at a given throat Mach number and free-stream velocity, the diffusion velocity ratio increases, up to a limit at which separation occurs, as the angle of attack increases. From experimental data for 30.5-centimeter-diameter STOL model inlets, the diffusion-velocity-ratio limit was in the range 2.4 to 2.8. This means that, if the diffusion velocity ratio is above 2.8, the inlet flow will probably separate; if it is below 2.4, the flow will probably stay attached; in between these limits is a band of uncertainty. Similarly, the peak Mach number limit was in the range of 1.4 to 1.6 and occurred at average throat Mach numbers above 0.6. The inlets presently under study were analyzed at a throat Mach number of around 0.4 and therefore can be expected to be diffusion-velocity-ratio limited.

The limiting value of diffusion velocity ratio is expected to increase with increasing inlet size or Reynolds numbers. This diffusion velocity ratio is one of the chief dependent parameters used herein to evaluate the tendency toward separation of the geometries studied.

A dependent parameter used to indicate the severity of the flow separation for the inlets that separate is the dimensionless distance x/D_{de} from the point of separation to the diffuser exit. The larger this distance, the more extensive the separation is likely to be. This parameter is obtained from the boundary-layer calculations and will be used in conjunction with the diffusion velocity ratios to evaluate the aerodynamic performance of the various geometries.

The final dependent parameters to be discussed herein are the dimensionless length L/D_{de}, maximum diameter D_{max}/D_{de}, and external surface area $4D_{max}L/D_{de}^2$. The latter is a simple geometric parameter that serves as a measure of the relative forward nacelle external surface area and hence the resulting weight and drag.

In summary, the dependent parameters presented herein are inlet surface-pressure distribution, diffusion velocity ratio, dimensionless distance to separation, and dimensionless length, diameter, and external surface area. The independent geometric variables are lip contraction ratio, lip major-to-minor axis ratio, diffuser-exit-area to throat-area ratio, diffuser wall angle, and diffuser wall shape (conic or cubic). All results are for the given flow condition: $M_0 = 0.18$, $\alpha = 60^{\circ}$, and diffuser-exit Mach number of 0.357.

Effect of Lip Contraction Ratio

The inlets considered in this section all have a cubic diffuser with a maximum wall angle of 8.7°, lip a/b ratio of 2.0, $A_{de}/A_t = 1.10$, and a drag-divergence Mach number of 0.8 (table I, inlets 1 to 3; and fig. 2).

Figure 9 shows the surface-pressure ratios as a function of dimensionless distance from the throat for the contraction ratios of 1.46, 1.56, and 1.69. For all the inlets the minimum pressure location (peak Mach number) occurred very near the highlight. Also, as the contraction ratio increased, the minimum pressure increased, and the wall static-pressure rise decreased. Most of the static-pressure rise occurs upstream of the throat; correspondingly, the diffuser pressure distributions are quite similar.

The value of diffusion velocity ratio is derived from the results of figure 9 and presented in table II and figure 10. The diffusion velocity ratio decreases greatly with increasing contraction ratio. While increasing contraction has a pronounced favorable effect on the diffusion velocity ratio, it also significantly increases the L/D_{de}, D_{max}/D_d (fig. 2) and the surface-area parameter (fig. 10). Therefore, the contraction ratio selected should be just large enough to maintain attached flow.

Effect of Lip Ellipse Major-to-Minor Axis Ratio

The inlets considered in this section all have cubic diffusers with maximum wall angles of 8.7°, lip contraction ratios of 1.56, $A_{de}/A_t = 1.10$, and drag-divergence Mach numbers of 0.8 (table I, inlets 1, 4, 5, and 6; and fig. 3). Figure 11 shows the surface-pressure ratio as a function of dimensionless distance from the throat for the lip a/b ratios of 2.00, 1.75, 1.50, and 1.25. As a/b decreases, the minimum pressure point (peak surface velocity and Mach number) moves closer to the throat, and, as a consequence, the adverse pressure gradient on the lip increases. It should be noted that the lip a/b ratio, like the previously discussed lip contraction ratio has little effect on the static-pressure distribution in the diffuser. The envelope of minimum surface pressure points has a maximum at a/b = 1.5. The diffusion velocity ratio is also lowest at about a/b = 1.5 (fig. 10). Reducing the a/b ratio reduces inlet length slightly (fig. 3) and the surface area parameter (fig. 10). Therefore, for the given flow condition, the diffusion velocity ratio parameter suggests that an a/b ratio of about 1.5 can be advantageous.

Effect of Diffuser-Exit-Area to Throat-Area Ratio

In this section the inlets all have cubic diffusers with maximum wall angles of 8.7°, lip a/b ratios of 2.0, lip contraction ratios of 1.56, and drag-divergence Mach numbers of 0.8 (table I, inlets 1, 7, and 8; and fig. 4).

Figure 12 shows the surface-pressure distribution as a function of dimensionless surface distance from the throat for diffuser-exit-area to throat-area ratios of 1.00, 1.10, and 1.14. These area ratios resulted in one-dimensional design throat Mach numbers of 0.6, 0.72, and 0.79, respectively, for a design diffuser-exit Mach number of 0.6. Note that equal throat and diffuser areas, $A_{de}/A_t = 1.0$, indicates equal Mach numbers at these locations. As indicated in figure 12, the value of the local surface pressure at the throat decreases in a manner related to the increase in one-dimensional Mach number as A_{de}/A_t increases. As can be seen from figure 10 and table II, the diffusion velocity ratio decreases with decreasing diffuser-exit-area to throat-area ratio. From figure 4 increasing A_{de}/A_t increases the inlet length L/D_{de} but decreases the maximum diameter D_{max}/D_{de}. The result of these two changes is to increase the surface-area parameter as shown in figure 10. Therefore, reducing A_{de}/A_t reduces both the diffusion velocity ratio and the external surface area (both favorable trends), suggesting a value of $A_{de}/A_t = 1.0$.

Effect of Diffuser Wall Angle

The inlets considered in this section all have internal lip a/b ratios of 2.0, contraction ratios of 1.56, $A_{de}/A_t = 1.10$, cubic wall diffusers, and drag-divergence Mach numbers of 0.8 (table I, inlets 1, 9, and 10; fig. 5). Figure 13 shows the surface-pressure ratio as a function of distance from the highlight for the 8.7°, 12°, and 14° maximum wall angles. Note that, because the centerbody geometry was held constant relative to the diffuser exit, the centerbody highlight location relative to the inlet throat changed with diffuser length as shown on the abscissa. As can be seen, the change in the diffusers has little effect on the surface static-pressure ratios upstream of $S/D_{de} = 0.15$, the upstream lip region. Close to the throat one can see a change. The larger wall angle inlets have a more gradual pressure rise than the smaller angle inlets between the throat and $S/D_{de} = 0.5$, an apparently contradictory effect. This, however, is due to the centerbody location for each inlet affecting the flow passage cross-sectional area.

Values of the diffusion ratio V_{max}/V_{min} for these configurations are independent of diffuser wall angle. But at the higher wall angles the minimum velocity is slightly less than the diffuser-exit velocity, and the location of the minimum velocity is just upstream of the diffuser exit. This effect is comparatively small for maximum diffuser

wall angles up to 14°, as can be seen by the small increase in V_{max}/V_{min} with diffuser wall angle in figure 10.

Figure 5 (left hand column) shows that increasing wall angle appreciably reduces the inlet length L/D_{de} but does not influence the maximum inlet diameter D_{max}/D_{de}. The reduction in inlet length significantly reduces the inlet external surface area with increasing wall angle as shown in figure 10. Thus, a more in-depth investigation of larger wall angles as possible optimum designs is indicated.

Effect of Diffuser Shape

The inlets considered in this section all have internal a/b ratios of 2.0, contraction ratios of 1.56, A_{de}/A_t of 1.10, conic diffusers, and drag-divergence Mach numbers of 0.8 (table I, inlets 11 to 13; and fig. 5). The effect of diffuser shape (i.e., conic or cubic) for maximum wall angles of 8.7°, 12°, and 14° on the internal static-pressure distribution is shown in figure 14. Since the conic diffuser is shorter than its corresponding cubic diffuser, the conic diffuser shows a steeper average pressure gradient. This steeper pressure gradient is due to the conic diffuser's reaching and maintaining its maximum wall angle a short distance from the throat. The cubic diffuser, on the other hand, gradually approaches its maximum value midway between the throat and the diffuser exit. It should also be noted that the pressure distribution in the conic-diffuser has an abrupt change in slope a short distance downstream of the throat. This change is due to the curvature discontinuity between the transition section and the conical (zero curvature) diffuser. (Refer to Geometric Variations section for details.) Geometric design refinements could smooth the pressure-distribution curve. The diffuser minimum pressure, like that for the cubic diffuser, is generally less than that at the diffuser exit and is upstream of the diffuser exit. Figure 10 shows that there is little difference in the diffusion velocity ratios of the two types of diffusers.

A comparison of the conic and cubic diffusers of figure 5 shows the conic inlets are short but have the same maximum diameters. Correspondingly, the conic diffusers have a smaller external surface area as shown in figure 10. Therefore, conic wall diffusers warrant consideration, especially for high A_{de}/A_t's and lower wall angles.

Circumferential Variation of Diffusion Velocity Ratio

The diffusion velocity ratios in table II are for the windward lip since that is the location of the most severe pressure gradients. However, for the three inlets that differ in contraction ratios (inlets 1, 10, and 11), the circumferential variation in diffusion velocity ratio is plotted in figure 15. As stated, the most severe diffusion ratio occurs

at the windward lip ($\theta = 0^{\circ}$). However, midway between the windward and leeward lips ($\theta = 90^{\circ}$), the diffusion velocity ratios for the three inlets are much reduced and almost equal. The dashed line in the figure is an example of a diffusion velocity ratio limit. For the 1.69 inlet no separation occurs. For the 1.56 inlet the extent of separation is about 35° on each side of the windward lip. For the 1.46 inlet the region of separation extends about 50° on each side of the windward lip. This angular extent information can be used to estimate the angular extent of boundary-layer control measures needed so that the inlets would not separate. Also, from figure 15 one can conclude that it is not necessary for an inlet to maintain a constant value of contraction ratio. It would be possible to design an inlet with a large contraction ratio on the windward lip that faired into a smaller value at the leeward lip without adversely affecting the aerodynamic performance of the inlet. In fact, figure 15 can be used to prescribe the circumferential variation of contraction ratio.

Scale Effects

Scale effects are those brought about by a change in Reynolds number due to a change in the size of the inlet. One of the effects of an increased size is that turbulent flow tends to remain attached for a relatively longer distance. This tendency can be seen in figure 16, which shows the comparison of the skin friction for inlet 1 (baseline inlet) between typical model scale (D = 50.8 cm) and full scale (D = 215.9 cm). The full-scale inlet exhibits a lower skin friction in the laminar region than the model, because of the increased Reynolds number. This result had been predicted in reference 7. However, once transition begins, the full-scale inlet reaches fully turbulent flow sooner and stays attached longer.

For the inlet geometries previously discussed, the effects of scale on separation location are shown in figure 17. As can be seen, the full-scale inlet exhibits delayed (better) separation characteristics (i.e., smaller x/D_{de}) than the corresponding model inlet. In fact, the full-scale inlet with $A_{de}/A_t = 1.0$ did not separate, while the model inlet did. Scale effect is considered to be most important for the following cases:

(1) Lower contraction ratios

(2) Higher a/b ratios

(Both of these factors give smaller highlight radii.)

(3) Lower diffuser-exit-area to throat area ratios

(4) Cubic and low wall angle diffusers.

SUMMARY OF RESULTS

The effect of internal lip and diffuser design on the aerodynamic performance was theoretically investigated for inlets of tilt-nacelle VTOL aircraft. The major geometric variables investigated were internal-lip contraction ratio, internal-lip major-to-minor axis ratio, diffuser-exit-area to throat-area ratio, and diffuser shape and maximum wall angle. The flow condition for each inlet analyzed was free-stream Mach number of 0.18, incidence angle of 60°, and diffuser-exit Mach number of 0.357. Some of the specific results based on both potential flow and boundary-layer analyses are

1. As contraction ratio is increased, the inlet becomes less likely to separate, but it also increases in size. Therefore, the contraction ratio selected should be the smallest that gives the required aerodynamic performance.

2. For a given contraction ratio, the lowest value of V_{max}/V_{min} occurred at an $a/b = 1.5$.

3. As diffuser-exit-area to throat-area ratio decreases, the inlet becomes less likely to separate and decreases in size. Therefore, the smaller values of A_{de}/A_t are desirable.

4. Increasing the maximum wall angle of the diffuser from 8.7° to 12° and 14° had little effect on the separation characteristics of the inlet, but did significantly reduce inlet size. Therefore, the larger angle diffuser walls should be considered when designing an inlet.

5. Increasing the scale of the inlet results in the tendency of the flow to remain attached for a relatively longer distance. The magnitude of the scale effect depends on the inlet geometry.

Lewis Research Center,
National Aeronautics and Space Administration,
Cleveland, Ohio, October 6, 1978,
505-05.

REFERENCES

1. Albers, James A.; Stockman, N. O.; and Hirn, John J.: Aerodynamic Analysis of Several High Throat Mach Number Inlets for the Quiet Clean Short-Haul Experimental Engine. NASA TM X-3183, 1975.

2. Hancock, J. P.; and Hinson, B. L.: Inlet Development for the L-500. AIAA Paper 69-448, June 1969.

3. Potonides, H. C.; Cea, R. A.; and Nelson, T. F.: Design and Experimental Studies of a Type A V/STOL Inlet. AIAA Paper 78-956, July 1978.

4. Stockman, Norbert O.: Potential and Viscous Flow in VTOL, STOL, or CTOL Propulsion Systems Inlets. AIAA Paper 75-1186, Sep. 1975.

5. Cebeci, Tuncer; and Bradshaw, Peter: Momentum Transfer in Boundary Layers. Hemisphere Publishing Corp., 1977.

6. Boles, M. A.; and Stockman, N. O.: Use of Experimental Separation Limits in the Theoretical Design of V/STOL Inlets. AIAA Paper 77-878, July 1977.

7. Chou, D. C.; Luidens, R. W.; and Stockman, N. O.: Prediction of Laminar and Turbulent Boundary Layer Flow Separation in V/STOL Engine Inlets. NASA TM X-73575, 1977.

TABLE I. - VTOL INLET GEOMETRIC PARAMETERS

Inlet	Contraction ratio, CR	Lip major-to-minor axis ratio, a/b	Diffuser wall shape	Maximum diffuser wall angle, λ_{max}, deg	Diffuser-exit-area to throat-area ratio, A_{de}/A_t	Inlet axial length to diffuser-exit diameter ratios, x/D_{de}
1	1.56	2.00	Cubic	8.7	1.10	0.96
2	1.46	2.00	↓	↓	↓	.93
3	1.69	2.00	↓	↓	↓	1.01
4	1.56	1.75	↓	↓	↓	.94
5	↓	1.50	↓	↓	↓	.91
6	↓	1.25	↓	↓	↓	.88
7	↓	2.00	↓	↓	1.00	.77
8	↓	↓	↓	↓	1.14	1.03
9	↓	↓	↓	12	1.10	.75
10	↓	↓	↓	14	↓	.67
11	↓	↓	Conic	8.7	↓	.77
12	↓	↓	Conic	12	↓	.66
13	↓	↓	Conic	14	↓	.62

TABLE II. - VTOL INLET POTENTIAL FLOW RESULTS

Inlet	Throat Mach number (a)	Maximum surface Mach number, M_{max}	Diffuser-exit surface Mach number, M_{de}	Surface diffusion ratio, V_{max}/V_{min}	Predicted boundary-layer behavior[b]
1	0.4	1.066	0.3472	2.90	Separated
2	↓	1.236	.3500	3.23	↓
3	↓	.917	.3455	2.57	↓
4	↓	1.037	.3476	2.83	↓
5	↓	1.004	.3482	2.76	↓
6	↓	1.037	.3483	2.82	↓
7	.357	.966	.3503	2.64	↓
8	.418	1.147	.3475	3.08	↓
9	.4	1.066	.3473	2.93	↓
10	↓	1.066	.3466	2.97	↓
11	↓	1.081	.3426	2.98	Uncertain
12	↓	1.082	.3463	2.97	Uncertain
13	↓	1.056	.3470	2.94	Separated

[a]Flow conditions: free-stream Mach number, 0.18; incidence angle, 60°; diffuser-exit Mach number, 0.357.

[b]Diffusion rate for attached region, ≤2.4; uncertain region, 2.4 - 2.8; separated region, >2.8.

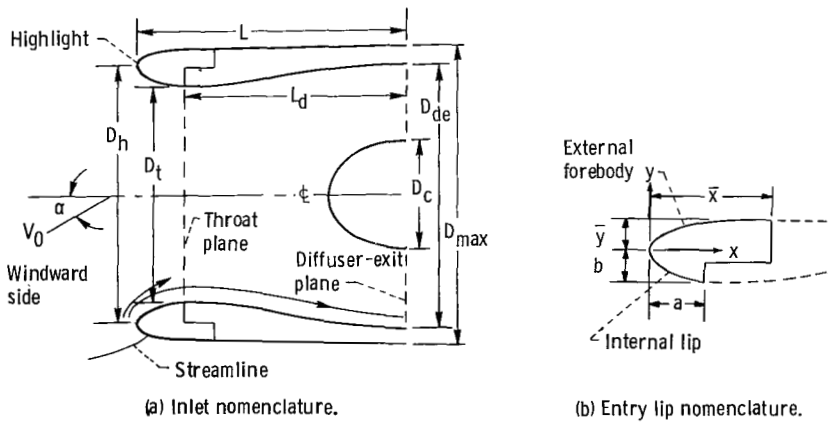

(a) Inlet nomenclature.

(b) Entry lip nomenclature.

Figure 1. - Inlet nomenclature.

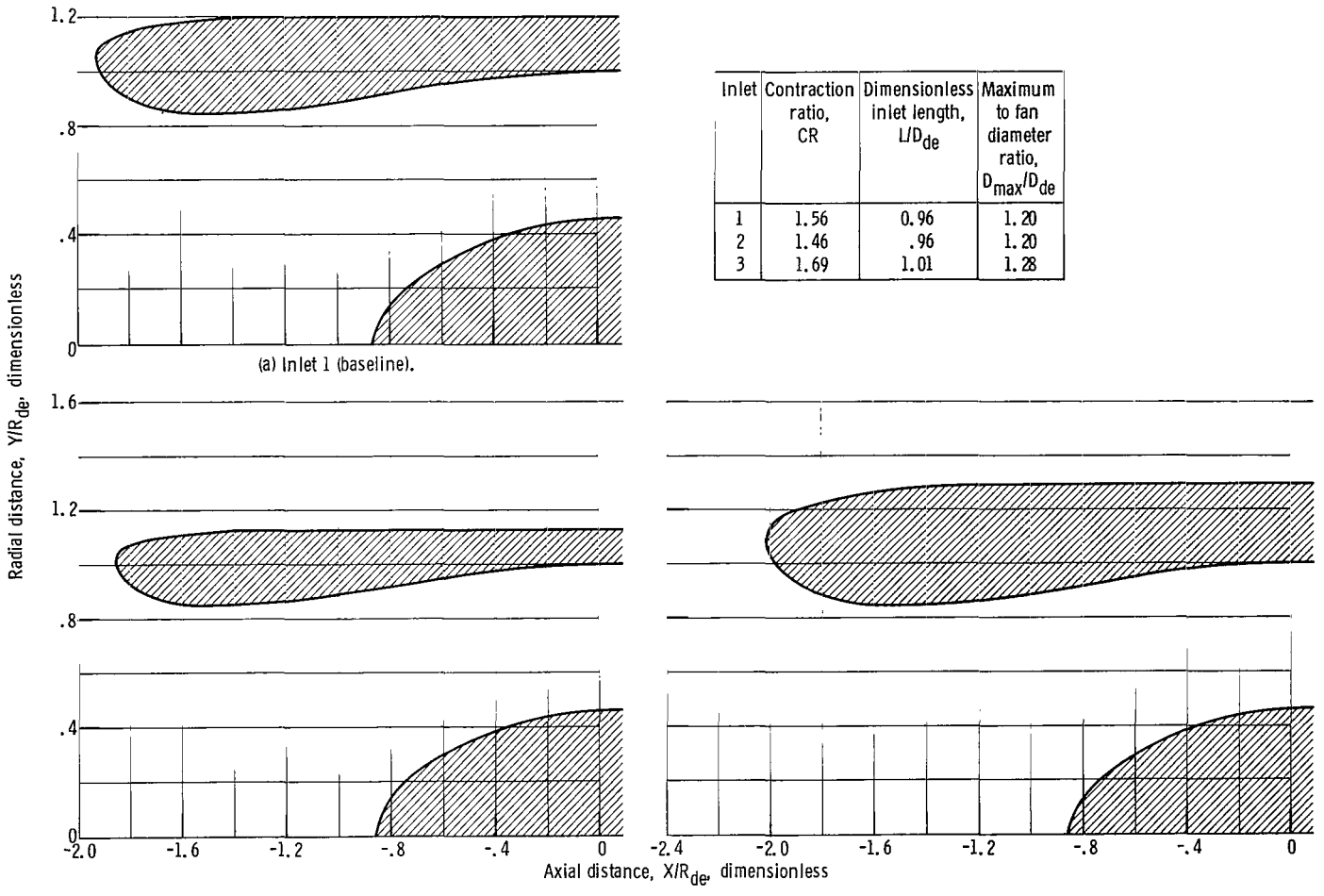

Inlet	Contraction ratio, CR	Dimensionless inlet length, L/D$_{de}$	Maximum to fan diameter ratio, D$_{max}$/D$_{de}$
1	1.56	0.96	1.20
2	1.46	.96	1.20
3	1.69	1.01	1.28

(a) Inlet 1 (baseline).

(b) Inlet 2.

(c) Inlet 3.

Figure 2. - Inlet geometry: variation of inlet contraction ratio. Cubic diffuser; maximum wall angle, 8.7°; lip major-to-minor axis ratio, 2.0; drag-divergence Mach number, 0.8; diffuser-exit-area to throat-area ratio, 1.10.

Inlet	Major to minor axis ratio, a/b	Dimensionless inlet length, L/D_{de}
1	2.00	0.96
4	1.75	.94
5	1.50	.91
6	1.25	.88

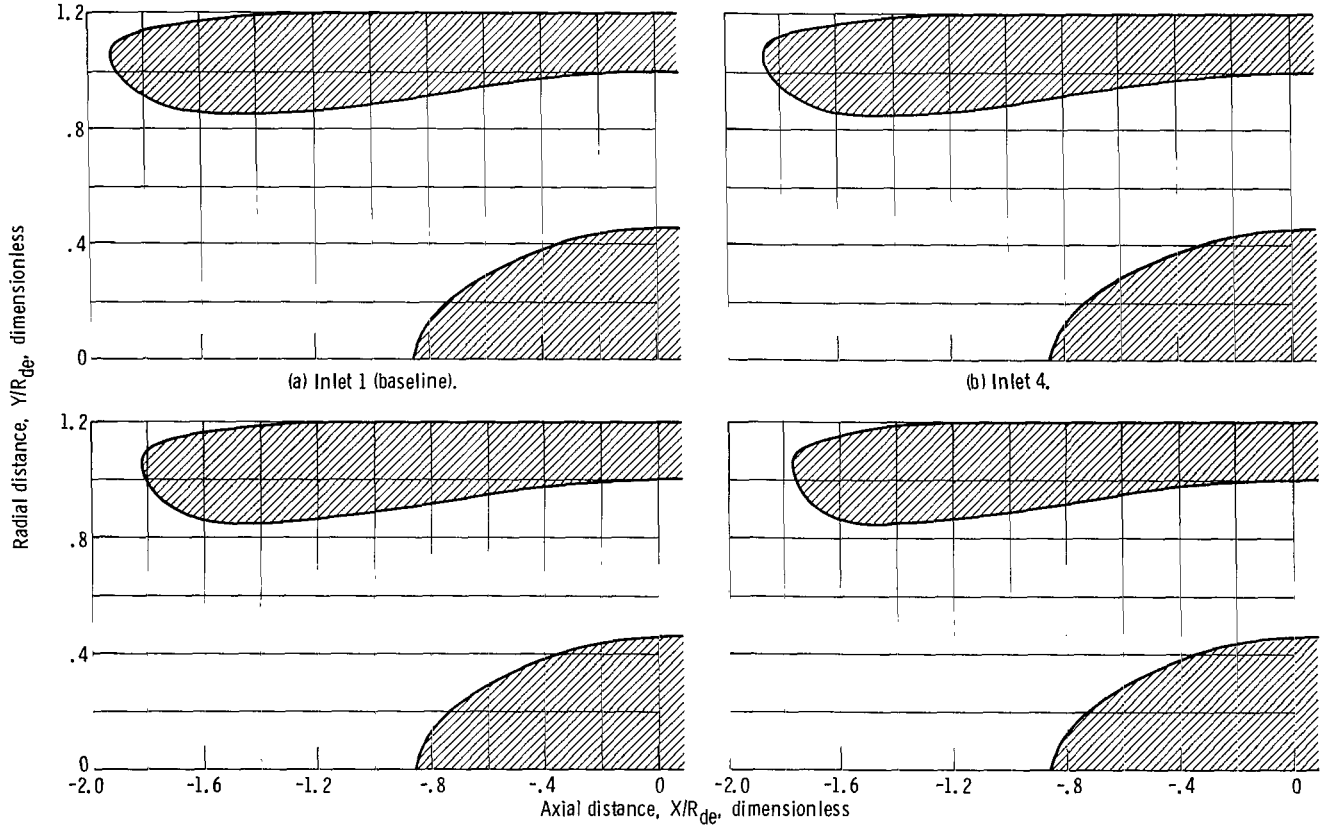

(a) Inlet 1 (baseline).

(b) Inlet 4.

(c) Inlet 5.

(d) Inlet 6.

Figure 3. - Inlet geometry: variation of internal lip major-to-minor axis ratio. Cubic diffuser; maximum wall angle, 8.7°; drag-divergence Mach number, 0.8; diffuser-exit-area to throat-area ratio, 1.10; contraction ratio, 1.56; maximum diameter to fan diameter ratio, 1.2.

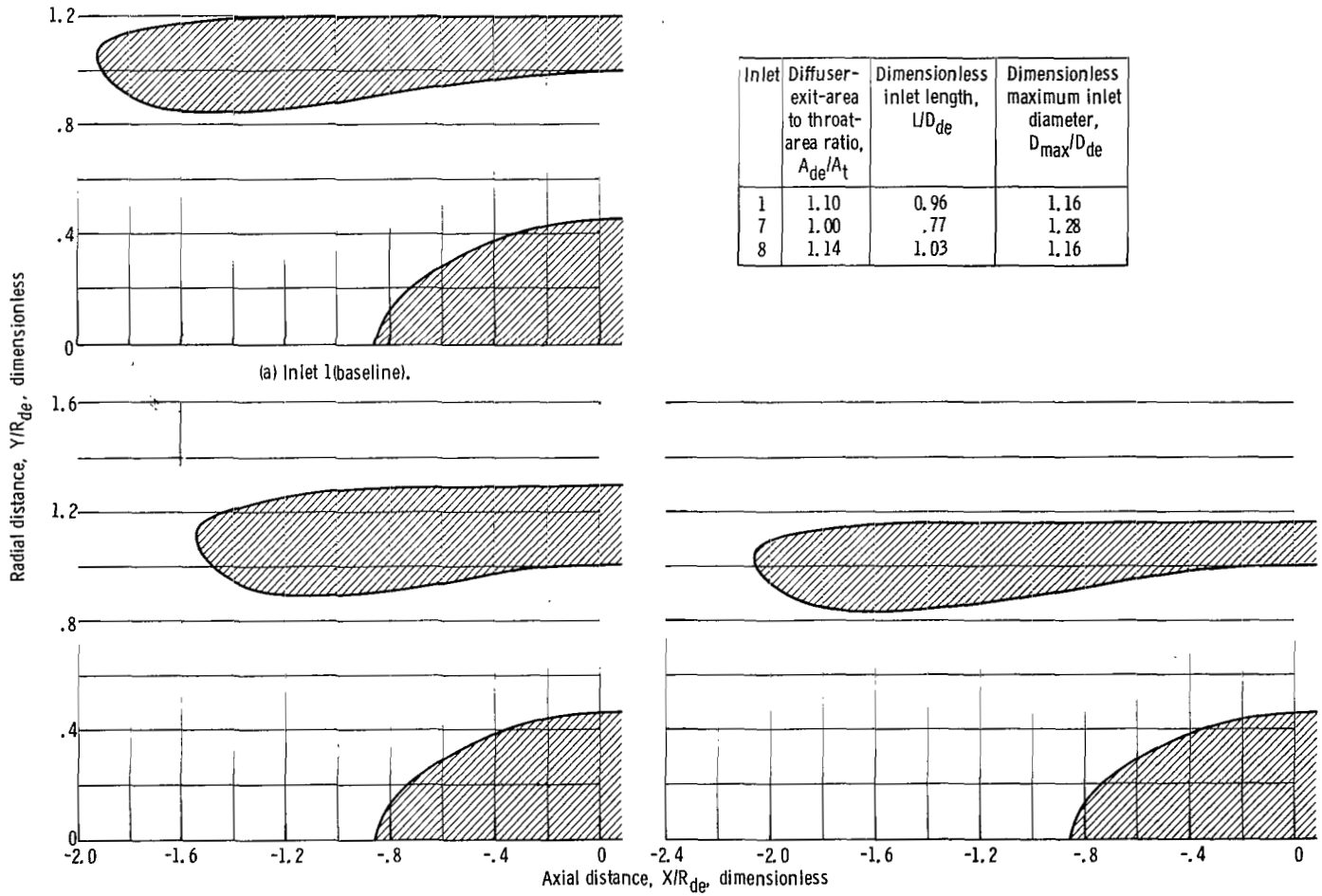

Inlet	Diffuser-exit-area to throat-area ratio, A_{de}/A_t	Dimensionless inlet length, L/D_{de}	Dimensionless maximum inlet diameter, D_{max}/D_{de}
1	1.10	0.96	1.16
7	1.00	.77	1.28
8	1.14	1.03	1.16

Figure 4. - Inlet geometry: variation of diffuser-exit-area to throat-area ratio. Cubic diffuser; maximum wall angle, 8.7^0; major-to-minor axis ratio, 2.0; drag-divergence Mach number, 0.8; contraction ratio, 1.56.

Inlet	Dimensionless inlet length, L/D_{de}	Maximum wall angle, λ_{max}, deg	Diffuser shape
1	0.96	8.7	Cubic
9	.75	12	
10	.67	14	
11	.77	8.7	Conic
12	.66	12	
13	.62	14	

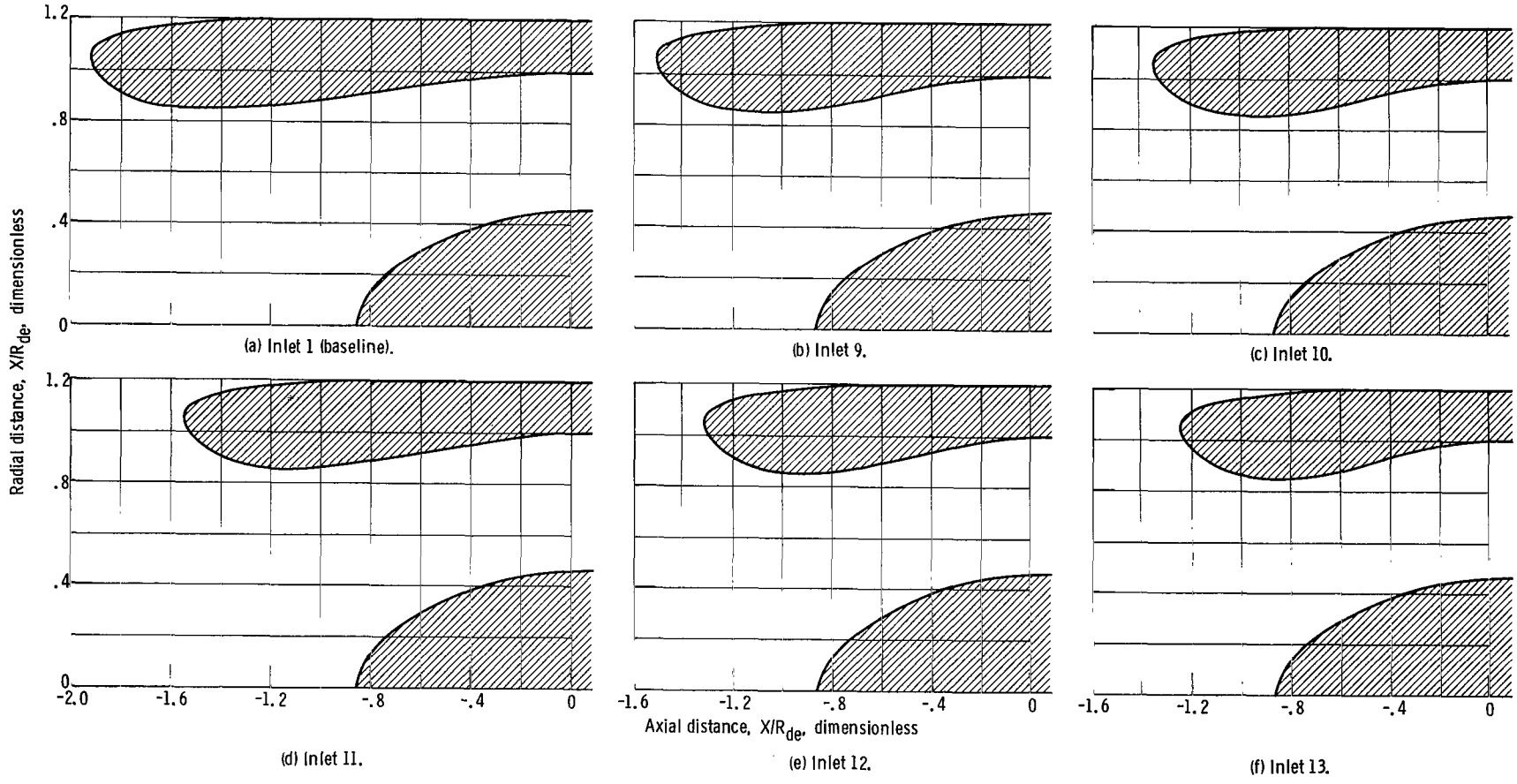

Figure 5. - Inlet geometry: variation of diffuser type and angle. Major-to-minor axis ratio, 2.0; contraction ratio, 1.56; drag-divergence Mach number; diffuser-exit-area to throat area ratio, 1.10; maximum diameter to fan diameter ratio, 1.2.

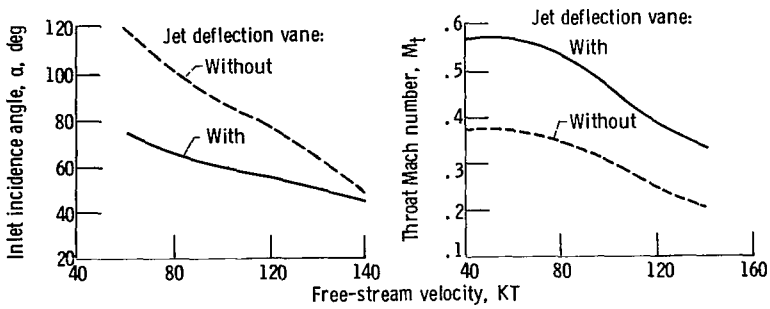

Figure 6. - Inlet operating requirements for tilt nacelle V/STOL aircraft.

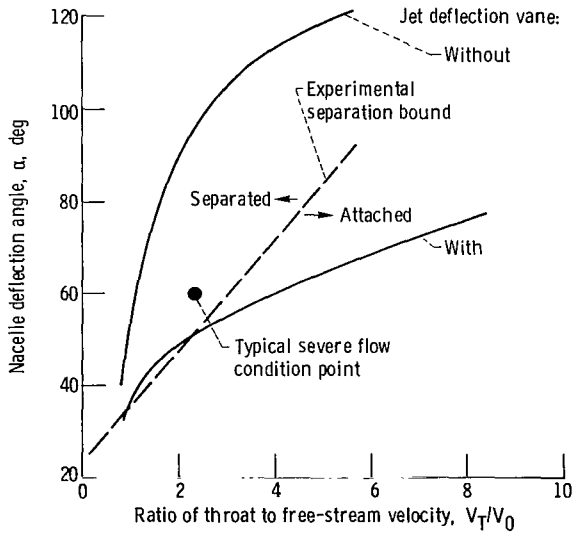

Figure 7. - Selection of critical condition for inlet analysis.

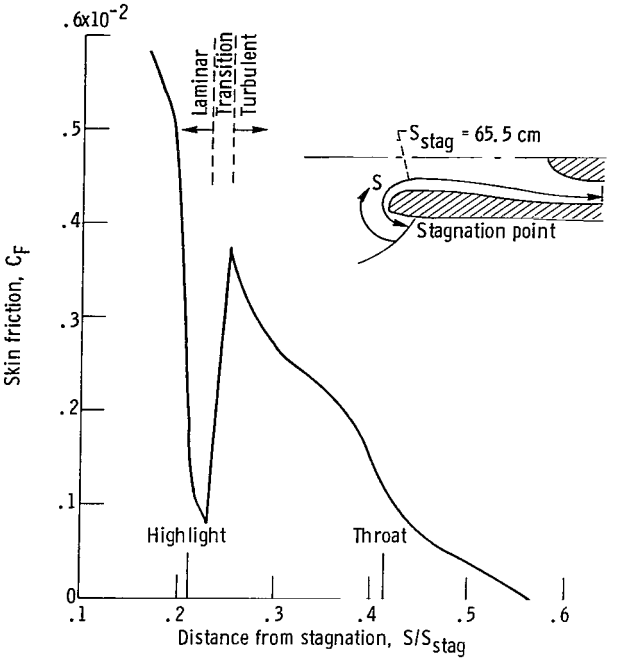

Figure 8. - Skin friction for baseline inlet (inlet 1). Fan diameter, D_f, 50.8 cm.

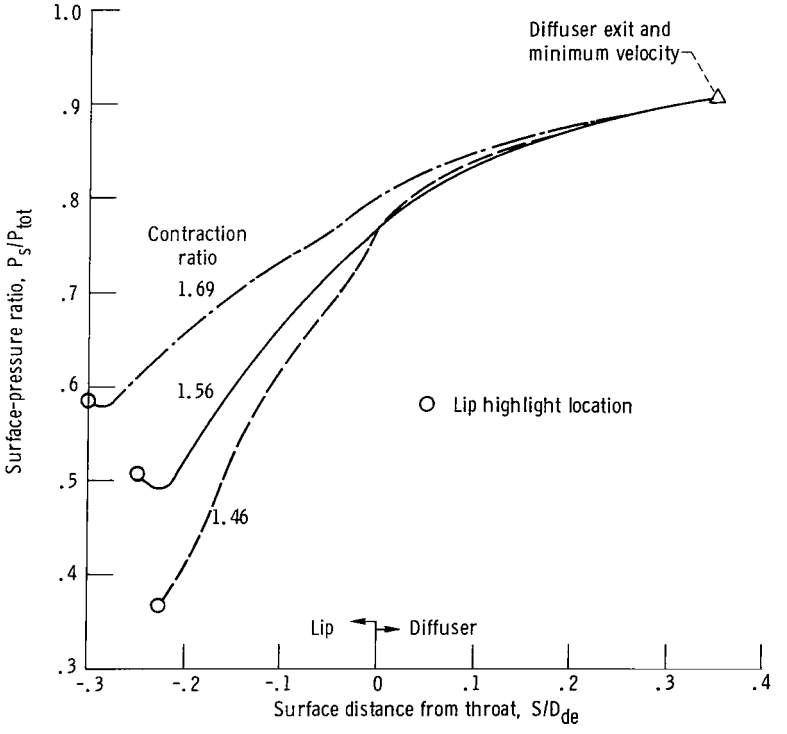

Figure 9. - Effect of contraction ratio on surface pressure ratio (see table I for geometric parameters).

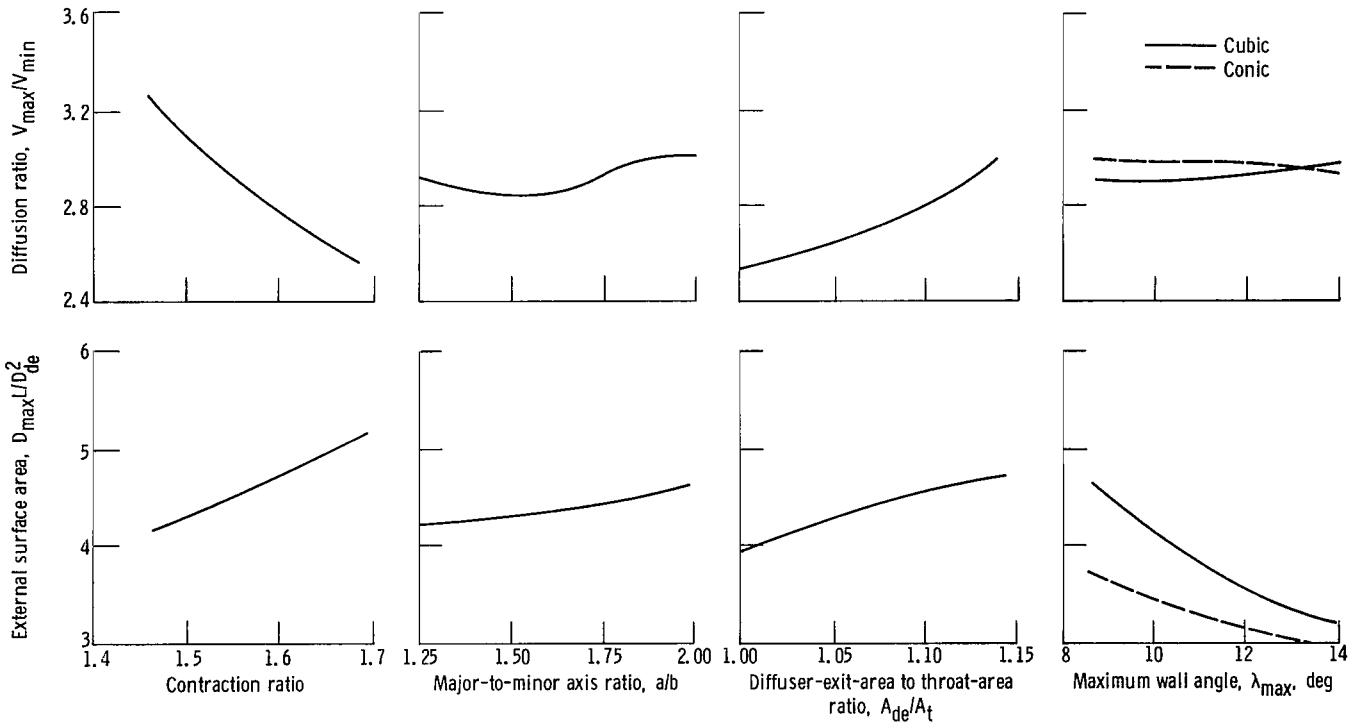

Figure 10. - Effect of geometric parameters on separation parameters and external surface area.

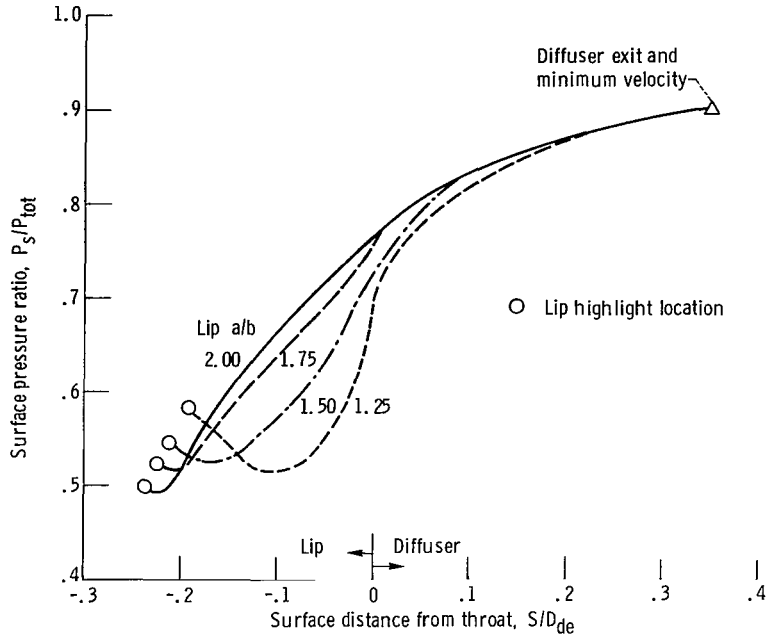

Figure 11. - Effect of internal lip major-to-minor axis ratio a/b on surface-pressure ratio (see table I for baseline parameters).

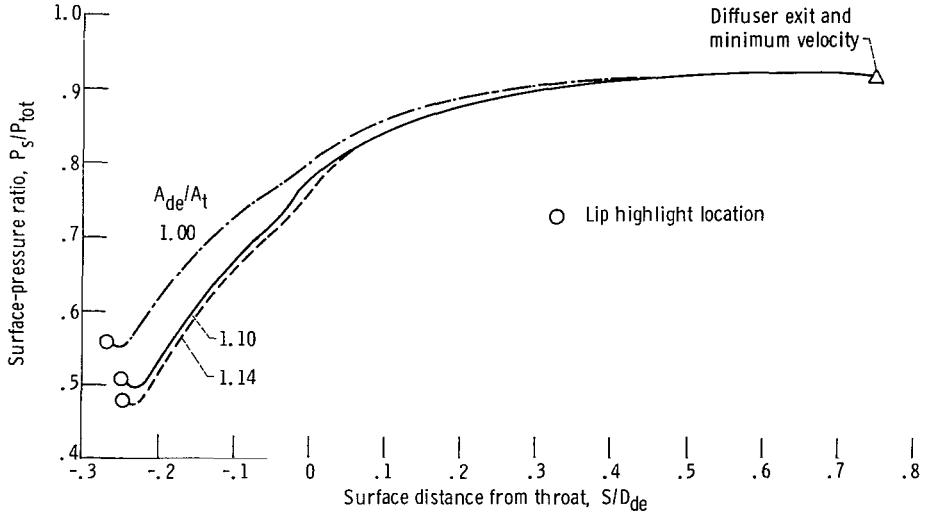

Figure 12. - Effect of diffuser-exit-area to throat-area ratio A_{de}/A_t on surface-pressure ratio (see table I).

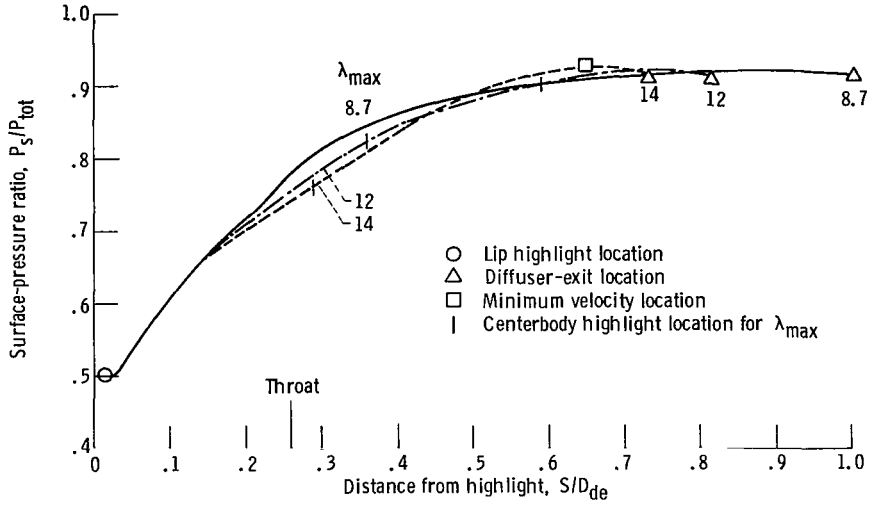

Figure 13. - Effect of maximum diffuser wall angle λ_{max} (cubic diffuser) on surface-pressure ratio. (See table I for baseline parameters.)

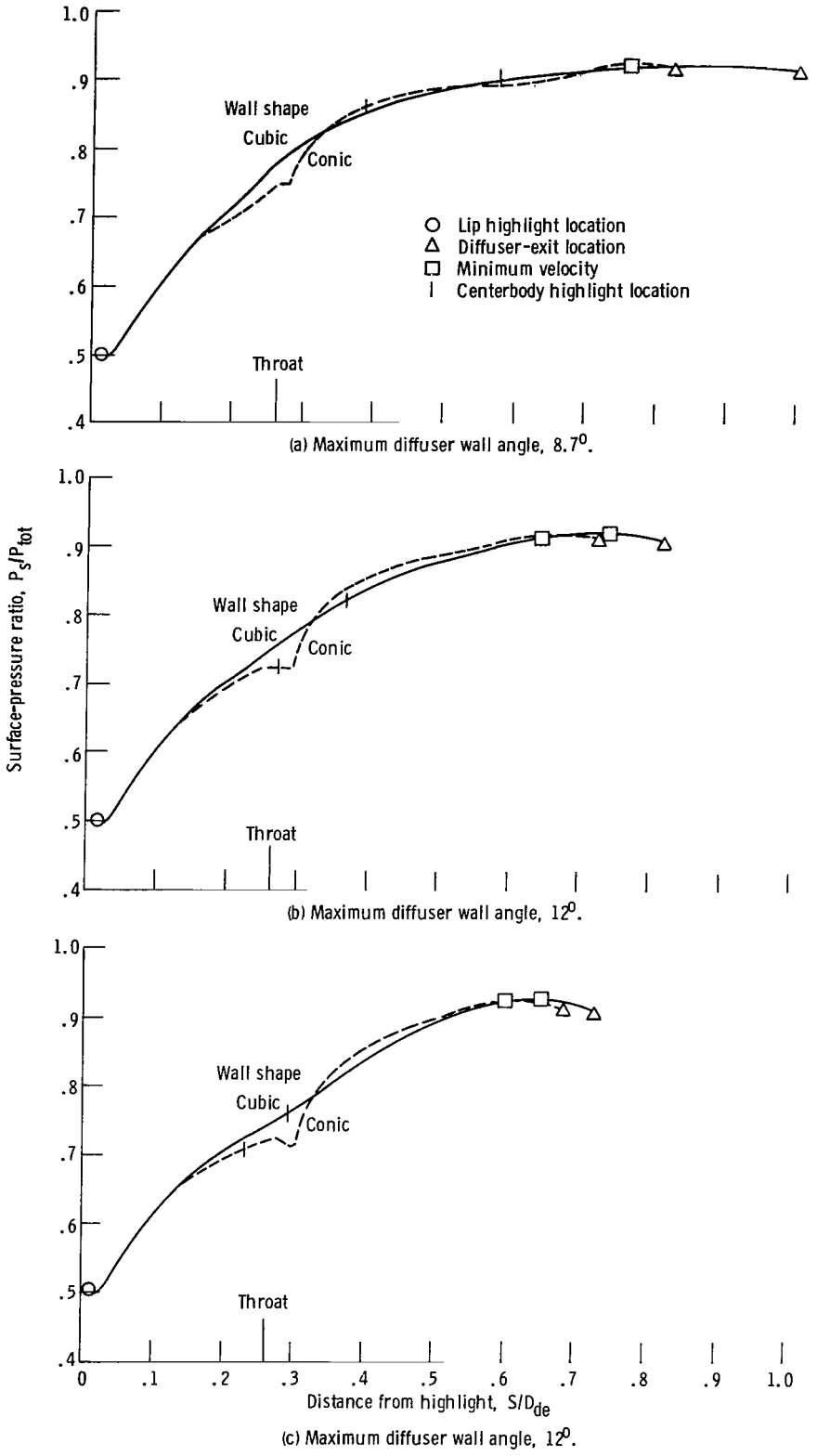

Figure 14. - Effect of diffuser wall shape on surface pressure ratio (see table I for baseline parameters).

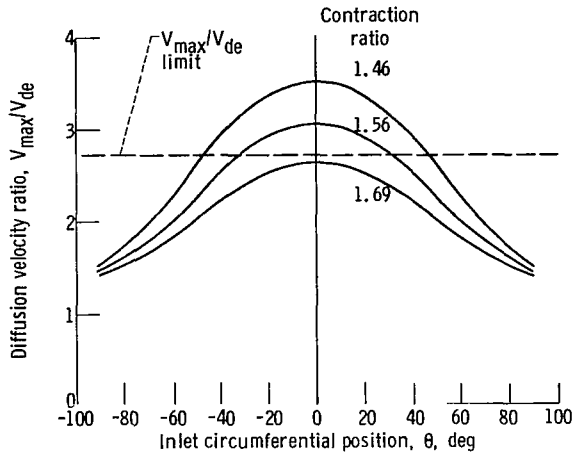

Figure 15. - Circumferential variation of diffusion velocity ratio around windward lip ($\theta = 0^{o}$). Lip major-to-minor axis ratio, 2.0; cubic diffuser; maximum wall angle, 8.7^{o}; design throat Mach number, 0.72; drag divergence Mach number, 0.80; free-stream Mach number, 0.18; incidence angle, 60^{o}; diffuser-exit Mach number, 0.357.

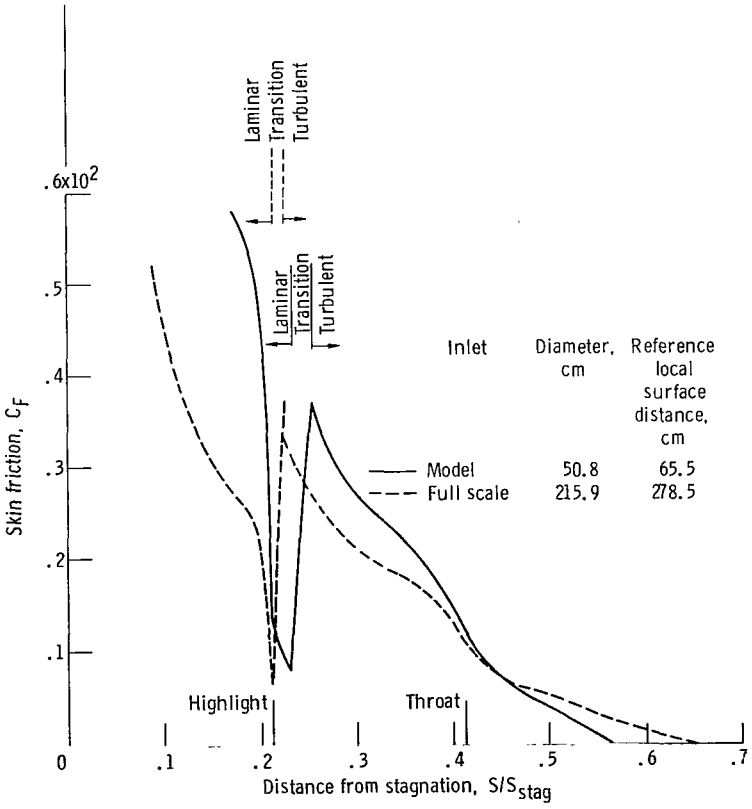

Figure 16. - Effect of scaling on skin friction for baseline inlet (inlet 1).

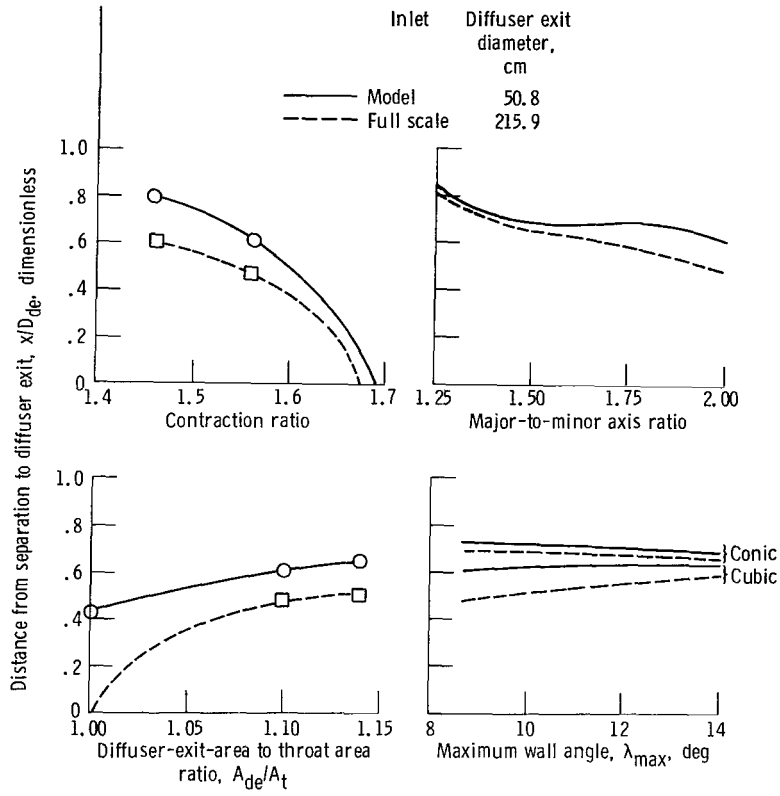

Figure 17. - Effect of geometric parameters and scaling on separation parameter.

1. Report No.	2. Government Accession No.	3. Recipient's Catalog No.
NASA TP-1380		

4. Title and Subtitle
THEORETICAL STUDY OF VTOL TILT-NACELLE AXISYMMETRIC INLET GEOMETRIES

5. Report Date
January 1979

6. Performing Organization Code

7. Author(s)
J. Dennis Hawk and Norbert O. Stockman

8. Performing Organization Report No.
E-9756

9. Performing Organization Name and Address
National Aeronautics and Space Administration
Lewis Research Center
Cleveland, Ohio 44135

10. Work Unit No.
505-05

11. Contract or Grant No.

12. Sponsoring Agency Name and Address
National Aeronautics and Space Administration
Washington, D.C. 20546

13. Type of Report and Period Covered
Technical Paper

14. Sponsoring Agency Code

15. Supplementary Notes

16. Abstract

This report presents a systematic theoretical study of VTOL tilt-nacelle inlet design parameters. The parameters considered are internal-lip contraction ratio, internal-lip major-to-minor axis ratio, diffuser-exit-area to throat-area ratio, and maximum diffuser wall angle and shape. Each of the inlets presented herein was analyzed at the same given flow condition of free-stream velocity, angle between the free stream and centerline of the inlet, and diffuser-exit Mach number. The effects of these geometric parameters on surface static-pressure distribution, peak surface Mach number, diffusion velocity ratio, and tendency for the inlet flow to separate are presented.

17. Key Words (Suggested by Author(s))	18. Distribution Statement
Inlet flow Engine inlets Nacelles V/STOL aircraft	Unclassified - unlimited STAR Category 02

19. Security Classif. (of this report)	20. Security Classif. (of this page)	21. No. of Pages	22. Price*
Unclassified	Unclassified	28	A03

* For sale by the National Technical Information Service, Springfield, Virginia 22161

NASA-Langley, 1979

National Aeronautics and
Space Administration

Washington, D.C.
20546

Official Business
Penalty for Private Use, $300

THIRD-CLASS BULK RATE

Postage and Fees Paid
National Aeronautics and
Space Administration
NASA-451

6 1 1U,A, 010879 S00903DS
DEPT OF THE AIR FORCE
AF WEAPONS LABORATORY
ATTN: TECHNICAL LIBRARY (SUL)
KIRTLAND AFB NM 87117

NASA

POSTMASTER: If Undeliverable (Section 158 Postal Manual) Do Not Return